Theory of optical spectra in a magnetic field in doped semiconductor quantum wells: Impurity-induced broadening and transitions

S. K. Lyo
Sandia National Laboratories, Albuquerque, New Mexico 87185
(Received 23 January 1989; revised manuscript received 1 May 1989)

The effect of carrier-impurity interactions on luminescence- and excitation-spectroscopy line shapes and the Landau-level spectral density in a strong quantizing magnetic field is examined in modulation-doped semiconductor quantum wells. The line-shape function is obtained by summing the "ladder diagrams," extending our previous "one-rung" approximation. Apart from yielding a line broadening, the carrier-impurity interaction is found to induce off-diagonal transitions (ODT) ($n \rightarrow n'$; $n' \neq n$) between the Landau levels in the conduction and valence bands, breaking the usual $n \rightarrow n$ selection rule. Here the first and second integers indicate the Landau quantum numbers in the conduction (valence) and valence (conduction) bands, respectively, for luminescence (excitation), for example, in an n-type system. The Landau-level spectral density (essential for obtaining the line-shape functions) is investigated by a self-consistent Born approximation which includes inter-Landau-level impurity scattering. The theory is applied to an n-type strained $In_xGa_{1-x}As/GaAs$ quantum well, where optical transitions arise between the conduction band and the strain-split in-plane "light-hole" band. For excitation spectra, the theory predicts that ODT introduce lines below the usual $n_F \rightarrow n_F$ threshold transition as well as satellite lines between the usual main $n \rightarrow n$ lines above the threshold (i.e., $n \geq n_F$). Here n_F is the quantum number of the lowest-lying empty or partially filled conduction-band Landau level. The luminescence line shape is dominated by ODT $1,2,\ldots \rightarrow 0$ (in addition to the main $0 \rightarrow 0$ transition) at low temperatures and by the usual $n \rightarrow n$ transitions at high temperatures. The accuracy of the "one-rung" approximation is assessed.

I. INTRODUCTION

Excitation and luminescence spectra yield rich information about electronic structure, doping configurations, and scattering dynamics in doped semiconductor quantum-well structures.[1] It was shown recently that Coulomb interactions between the carriers and ionized impurities (i.e., donors or acceptors in the doping layers) explain the low-temperature photoluminescence and magnetoluminescence line shapes in high-quality modulation-doped single-quantum-well $In_xGa_{1-x}As/GaAs$ samples with negligible fluctuations in the well width and a small inhomogeneous broadening.[1,2] A "single-rung" approximation was employed for the self-energy part of the photon propagators (responsible for the luminescence line shape). Recently Bauer and Ando calculated luminescence line shapes in $GaAs/Al_xGa_{1-x}As$ quantum wells, using a ladder approximation.[3] While the ladder approximation is in principle superior to the single-rung approximation, in the absence of an external magnetic field it was necessary to assume δ-function potentials for carrier-impurity interactions in order to sum the ladder series.[3] On the other hand, the one-rung approximation is more convenient in the sense that realistic potentials can be treated.[1] For magnetoluminescence, Bauer and Ando[3] summed the ladder series for arbitrary interaction potentials in the extreme quantum limit (i.e., with only the ground Landau level occupied) at zero temperature.[3]

The purpose of this paper is threefold. First, we establish a formalism for the line shape of magnetoluminescence by summing the ladder diagram exactly for arbitrary carrier-impurity potentials with an arbitrary Landau-level filling at finite temperatures in strong magnetic fields. Our results yield a new class of optical transitions which are absent in the extreme quantum limit.[3] Second, we use this result to calculate the effect of carrier-impurity interactions on the excitation spectra. In this paper the excitation line shape is defined as the photon-absorption rate as a function of the photon energy, with the photons being absorbed as a result of creating electron-hole pairs. We predict some new features which are induced by carrier-impurity interactions and propose an experimental verification of these effects. Third, we assess the accuracy of the one-rung approximation as compared to the ladder approximation. We find that the one-rung approximation is fairly accurate for both luminescence and excitation spectra. We also calculate the Landau-level spectral broadening and tailing (essential for obtaining the line-shape functions) by employing a self-consistent Born approximation which includes inter-Landau-level impurity scattering.

In our model, optical transitions occur between the conduction band (assumed to be degenerate with n-type-doping and with only the ground sublevel populated) and in-plane "light-hole" (i.e., $|\frac{3}{2},\pm\frac{3}{2}\rangle$) band. The in-plane "heavy-hole" (i.e., $|\frac{3}{2},\pm\frac{1}{2}\rangle$) band is assumed to be far away from the band edge due to biaxial strain arising from lattice mismatch and is not considered.

In a strong magnetic field B, the carriers are quantized

into several discrete low-lying Landau orbits ($n=0,1,\ldots$). As a result, various interband optical transitions and their mechanisms can be more conveniently identified and investigated than in the continuum situation (i.e., in the absence of the field). For example, Lyo, Jones, and Klem[2] recently demonstrated the existence of the impurity-induced line-shifting and -broadening mechanism (i.e., indirect processes) proposed for photoluminescence phenomena[1] by presenting evidence of breaking of the usual selection rule for magnetoluminescence:[2] They showed, in an n-type strained $In_xGa_{1-x}As/GaAs$ quantum well (where only in-plane light holes are present due to strain-induced heavy–light-hole splitting), that the off-diagonal transitions (ODT) between the low-lying Landau levels $n=1,2,\ldots$ in the conduction band and the ground level $n=0$ in the valence band give (together with the main $0\rightarrow 0$ transition) major contributions to the magnetoluminescence line shape at low temperatures. At high temperatures, the line shape is dominated by the usual direct (i.e., $n\rightarrow n$) transitions (DT). This temperature-dependent crossover arises from the fact that at a sufficiently high magnetic field all the holes are in the ground level at low temperatures (and at low laser power), while higher levels are populated at high temperatures.

ODT occur through higher-order processes: For example, the $1\rightarrow 0$ transition, illustrated by a dashed arrow pointed downward on the left side in Fig. 1, utilizes the fact that the initial electron level $n=1$ (hole ground level $n=0$) is admixed with the electron ground level $n=0$ (hole level $n=1$) through impurity-electron (hole) matrix element. As a result, the initial electron (hole) state has a small component which overlaps with the initial hole (electron) state, yielding ODT. These processes are schematically illustrated in Fig. 2. Electron-hole recombination processes representing ODT and DT are illustrated in Fig. 1 by dashed and solid arrows pointed downward, respectively. In this paper we assume that the first

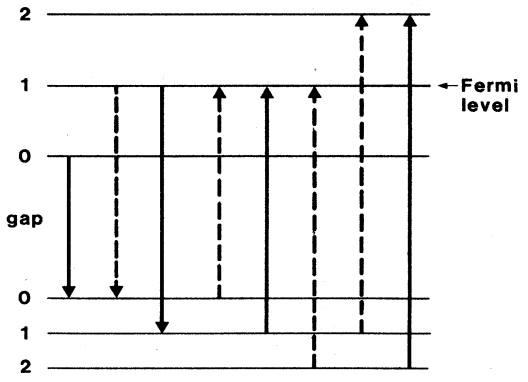

FIG. 1. Solid and dashed arrows connecting electron and hole Landau levels (horizontal lines) indicate DT and ODT for luminescence (directed downward) and excitation (directed upward). The Fermi level is at the electron level $n=1$, which is half filled.

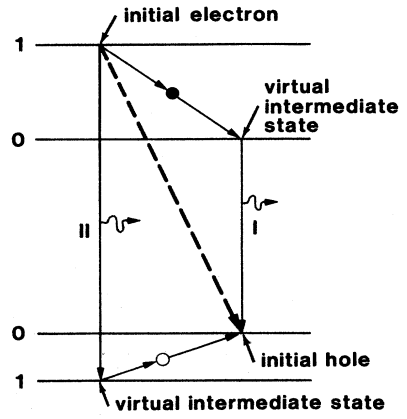

FIG. 2. Schematic illustration of ODT arising from the one-rung correction. In channel I (II), the initial electron (hole) is admixed, through electron (hole)-impurity scattering denoted by a solid (empty) circle to an intermediate state which has a full overlap with the initial hole (electron) state. The vertical arrows with wiggly curves attached denote coupling with the photon field and the broken arrow the resonant photons.

electron Landau level ($n_c=1$) is half filled at zero temperature for illustrations and applications. The simple one-step-admixing picture for ODT corresponds to a one-rung approximation.[2] Multilevel-admixing effects are considered by employing a ladder approximation.

Also, photons with energies corresponding to ODT are emitted in DT processes. In the $0\rightarrow 0$ transition [Fig. 3(a)], for example, a majority of the resonant photons have the energy corresponding to the energy difference between the ground-state conduction- and valence-band Landau levels, because the spectral densities have primary peaks at the ground levels. However, the spectral density of the ground electron level ($n_c=0$) has smaller but nonvanishing evanescent peaks at neighboring levels as is illustrated in Fig. 3(a). Of particular interest in the example in Fig. 3(a) is the secondary peak at $n_c=1$ which allows emission of photons (indicated by a downward dashed line) with the energy corresponding to the $1\rightarrow 0$ transition. This kind of process arising from spectral-density tailing effects will also be defined as ODT and will be discussed in more detail later. ODT originate in a similar way in excitation spectroscopy.

We find only an insignificant difference between the results of the ladder and one-rung approximations for both luminescence and excitation spectra. For luminescence spectra, we obtain the behavior consistent with the data explained above. For excitation spectra, our result predicts new ODT-induced lines below the threshold transitions (corresponding to $n_F\rightarrow n_F$ transitions) and satellite lines (also induced by ODT) between the main $n\rightarrow n$ lines above the threshold. Here n_F denotes the lowest-lying empty or partially empty conduction-band Landau level. Excitation processes corresponding to ODT and DT are illustrated in Fig. 1 by dashed and solid arrows pointed upward, respectively. The $1\rightarrow 1$ transition is the usual excitation threshold.

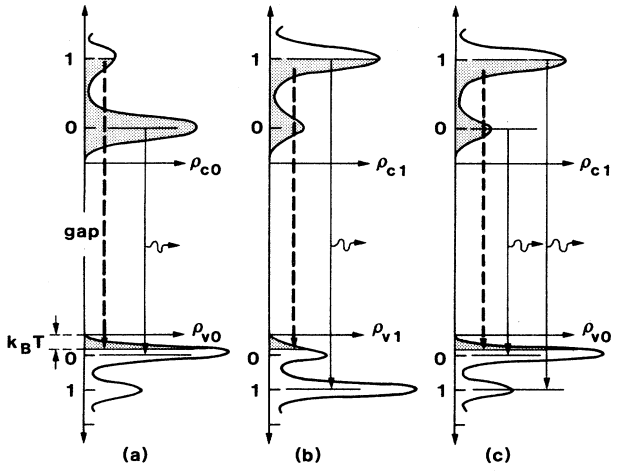

FIG. 3. Schematic illustration of ODT. In (a) and (b), electron and hole levels are coupled via $0\rightarrow 0$ and $1\rightarrow 1$ DT by the photon field (solid vertical arrows with wiggly curves attached). Shaded regions denote carrier population. $1\rightarrow 0$ photons (dashed arrows) are emitted owing to impurity-induced tailing of the spectral densities ρ_{c0} and ρ_{v1} in (a) and (b), respectively. The mechanism in (c) is the same as that given in Fig. 2.

II. FORMALISM

The line-shape function for luminescence is given by a dipole-dipole correlation function given in Ref. 1, which yields apart from a multiplicative constant

$$F(\omega)=g\Theta(\omega)\times\mathrm{Re}\int_0^{\omega} f(\zeta-\mu_v)f(\omega-\zeta-\mu_c)\times\sum_{nn'}\langle n|[L(\zeta-i0,\omega-\zeta+i0)-L(\zeta+i0,\omega-\zeta+i0)]|n'\rangle d\zeta , \quad (1)$$

where $g=1/(2\pi l^2)$, $l=(\hbar c/eB)^{1/2}$ is the classical magnetic length, $\Theta(\omega)$ the unit-step function, ω the photon energy minus the renormalized band gap, μ_c (μ_v) the chemical potential for electrons (holes) and $f(x)=1/[\exp(x)+1]$. The state vectors $|n\rangle$ represent the harmonic part (normalized) of the Landau wave functions in an asymmetric gauge and Re denotes the real part. The excitation line shape is obtained from (1) by replacing the product of the Fermi functions by $1-f(\omega-\zeta-\mu_c)$. The external-field vertex part $L^{\pm}=L(\zeta\pm i0,\omega-\zeta+i0)$ in (1) is given in a ladder approximation shown in Fig. 4 by

$$L^{\pm}=B^{\pm}+B^{\pm}U^{cv}B^{\pm}+B^{\pm}U^{cv}B^{\pm}U^{cv}B^{\pm}+\cdots . \quad (2)$$

The diagrammatic rules for carriers in quantizing magnetic fields are established in Ref. 4. Each rung in Fig. 4 is proportional to the number of impurities N_I and the product of electron-impurity and hole-impurity potentials averaged over the impurity distribution [denoted by angular brackets in (3a)]:

$$\langle n|U^{cv}|n'\rangle=N_I\langle V_q^c V_q^v\rangle\frac{n_<!}{n_>!}\times\exp(-\tilde{q}^2)\tilde{q}^{2\Delta n}[L_{n_<}^{\Delta n}(\tilde{q}^2)]^2 , \quad (3a)$$

where $\tilde{q}^2=(ql)^2/2$, V_q^{α} is the q Fourier component of the impurity potential for α band, q the wave-vector transfer and $L_n^n(x)$ is the associated Laguerre polynomial.[4] The quantity $n_<$ ($n_>$) denotes the lesser (greater) of n and n' ($=0,1,\ldots$) and $\Delta n=n_>-n_<$. In (3a) V_q^{α} is given by

$$V_q^{\alpha}=\frac{2\pi Ze^2 s_{\alpha}}{\kappa q\varepsilon_q}\times(\Phi_q^{\alpha}(z_i)+(\varepsilon_q-1)\{\Phi_q^{\alpha}(z_i)-[F_{\alpha c}(q)/F_{cc}(q)]\Phi_q^c(z_i)\}) , \quad (3b)$$

where $\varepsilon_q=1+sF_{cc}(q)q^{-1}$, $s_c=-1$ for electrons, and $s_v=1$ for holes. The quantities κ, Ze, and $s=2\pi e^2\Pi_q/\kappa$ denote the dielectric constant, ionic charge, and the screening constant in the random-phase approximation, respectively. The quantity Π_q is given by [5]

$$\Pi_q=\exp(-\tilde{q}^2)[L_{n_F}(\tilde{q}^2)]^2 D(\epsilon_F) , \quad (3c)$$

where $D(\epsilon_F)$ is the density of states of the majority carriers at the Fermi energy. The form factor is given by

$$F_{\alpha\beta}(q)=\int\int\phi_{\alpha}(z)^2\phi_{\beta}(z')^2\exp(-q|z-z'|)dz\,dz' \quad (3d)$$

and accounts for the finite extent of the wave function in the growth (z) direction. Here $\phi_{\alpha}(z)$ is the confinement wave function. Finally, the quantity $\Phi_q^{\alpha}(z_i)$ in (3b) is given by

$$\Phi_q^{\alpha}(z_i)=\int[\phi_{\alpha}(z)]^2\exp(-q|z-z_i|)dz , \quad (3e)$$

where z_i is the impurity position. The quantity in the curly brackets of (3b) vanishes for electrons ($\alpha=c$). For holes ($\alpha=v$), it is small when electrons and holes have similar density distributions (corresponding to a well-confined situation) vanishing in the particle-in-a-box limit.[6]

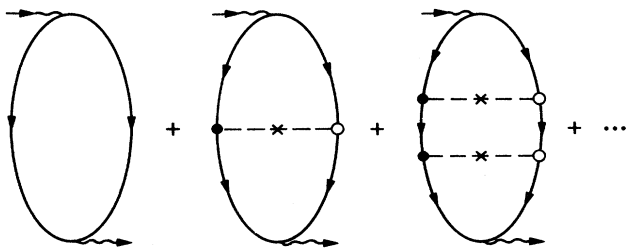

FIG. 4. Ladder diagrams contributing to luminescence and excitation. Directed solid lines denote electron (left side) and hole (right side) propagators and the wiggly lines the external photon propagators. The solid and empty circles indicate electron-impurity and hole-impurity interactions. The crosses represent a single-impurity averaging.

Each rung in Fig. 4 is also accompanied by a pair of electron-hole propagators:

$$\langle n|B^{\pm}|n'\rangle=\delta_{n,n'}G_{vn}(\zeta\pm i0)G_{cn}(\omega-\zeta+i0)\ , \tag{4}$$

where $\delta_{n,n'}$ is Kronecker's delta,

$$G_{\alpha n}(\zeta\pm i0)=\frac{1}{\zeta-\epsilon_{\alpha n}-S_{\alpha n}(\zeta\pm i0)}$$
$$\equiv R_{\alpha n}(\zeta)\mp iI_{\alpha n}(\zeta)\ , \tag{5}$$

$\epsilon_{\alpha n}=(n+\frac{1}{2})\hbar\omega_{\alpha}$ and $\omega_{\alpha}=eB/(m_{\alpha}^{*}c)$. The spin splitting is ignored. Here $m_{c,v}^{*}$ is the effective mass of electrons and holes, $S_{\alpha n}$ the self-energy part, and $R_{\alpha n}$ ($I_{\alpha n}$) the real (imaginary) part of the Green's function.

The external vertex function (2) is summed, yielding

$$L^{\pm}=(1-B^{\pm}U^{cv})^{-1}B^{\pm}\ , \tag{6}$$

where the quantity 1 inside the parentheses indicates an identity matrix and $B^{\pm}$ and U^{cv} are square matrices defined in (4) and (3a), respectively. The size of the matrices can be chosen to be somewhat larger than the number of occupied levels for the luminescence problem. For photoexcitation, it equals the number of levels participating in the transitions in a given photon-energy range. An arbitrary numerical accuracy can be achieved by increasing the size of the matrices. The finite complex matrix $1-B^{\pm}U^{cv}$ in the denominator of (6) is readily inverted. The final result is then given by (1) and Eqs. (3)–(6).

The present result constitutes an extension (as well as a more complete analysis) of our previous single-rung approximation for multilevel systems[2] to include the ladder sum. A single-rung approximation corresponds to expanding

$$(1-B^{\pm}U^{cv})^{-1}\approx 1+B^{\pm}U^{cv}\ , \tag{7}$$

which inserted in (6) and (1) yields

$$F(\omega)=2g\Theta(\omega)\int_0^{\omega}f(\zeta-\mu_v)f(\omega-\zeta-\mu_c)$$
$$\times\Big[\sum_n I_{vn}(\zeta)I_{cn}(\omega-\zeta)$$
$$+\sum_n\sum_m 2U_{nm}^{cv}[R_{cn}(\omega-\zeta)R_{vn}(\zeta)I_{cm}(\omega-\zeta)I_{vm}(\zeta)+I_{cn}(\omega-\zeta)R_{vn}(\zeta)R_{cm}(\omega-\zeta)I_{vm}(\zeta)]\Big]d\zeta\ . \tag{8}$$

The functions $R_{\alpha n}$ and $I_{\alpha n}$ are defined in (5). The DT contribution arises mainly from the first term in the large parentheses in (8), while ODT comes from the same term as well as from the second term in the square brackets therein.

III. GREEN'S FUNCTION AND THE SPECTRAL DENSITY

In the formalism presented in the previous section, the only undefined quantity is the self-energy part $S_{\alpha n}(\zeta\pm i0)$ of the Green's function $G_{\alpha n}(\zeta\pm i0)$. This quantity is obtained in the high-field limit by a self-consistent Born approximation which includes inter-Landau-level scattering. Contributions to the intensity come from the energy domain of ζ and $\omega-\zeta$, where the density of states is nonvanishing [i.e., $A_{\alpha m}\geq 0$ in (9)]. In this region we find (see the Appendix)

$$S_{\alpha n}(\zeta-i0)=\sum_m(\Gamma_{nm}^{\alpha}/\Gamma_{mm}^{\alpha})^2S_{\alpha m}^{0}(\zeta-i0)\Theta(A_{\alpha m})\ , \tag{9a}$$

where

$$S_{\alpha n}^{0}(\zeta-i0)=\tfrac{1}{2}(\zeta-\epsilon_{\alpha n}+\delta_{\alpha n}+i\sqrt{A_{\alpha n}})\ , \tag{9b}$$

$$A_{\alpha n}(\zeta)=(\Gamma_{nn}^{\alpha})^2-(\zeta-\epsilon_{\alpha n}-\delta_{\alpha n})^2\ , \tag{9c}$$

and the spectral shift

$$\delta_{\alpha n}(\zeta)=\tfrac{1}{4}{\sum_m}'\frac{(\Gamma_{nm}^{\alpha})^2}{\zeta-\epsilon_{\alpha m}} \tag{9d}$$

with $(\Gamma_{nm}^{\alpha})^2=4\langle n|U^{\alpha\alpha}|m\rangle$. In (9d), the prime on the summation symbol means excluding the diagonal term $m=n$. The results in (9) are valid when the Landau levels are well separated [i.e., $\xi^2\equiv(\Gamma_{nm}^{\alpha}/\hbar\omega_{\alpha})^2\ll 1$]. Equation (9) satisfies the normalization condition that the total number of states ($=2g$) per level is independent of the level broadening (see the Appendix).

In (9a), the contribution from $m=n$ arises from intra-Landau-level scattering[3] and the other terms from inter-Landau-level scattering. For the spectral density of the level n defined as

$$\rho_{\alpha n}(\zeta)=\frac{1}{\pi}I_{\alpha n}(\zeta)$$
$$=\frac{2}{\pi}\left[(\Gamma_{nn}^{\alpha})^{-2}\Theta(A_{\alpha n})\sqrt{A_{\alpha n}}\right.$$
$$\left.+\tfrac{1}{4}{\sum_m}'\frac{(\Gamma_{nm}^{\alpha}/\Gamma_{mm}^{\alpha})^2}{(\epsilon_{\alpha n}-\epsilon_{\alpha m})^2}\Theta(A_{\alpha m})\sqrt{A_{\alpha m}}\right]\ , \tag{10}$$

the interlevel scattering transfers some states from the main nth level to the neighboring levels [second term in (10)]. The total integrated spectral density of (10) is unity [see (A10) in the Appendix]. This tailing effect of the spectral density is schematically illustrated in Fig. 3 for the lowest two Landau levels of the conduction and valence bands. The magnitude of the spectral density at the secondary peaks at the neighboring levels is small ($\propto\xi^2$) as compared to the main peak. The density of states is obtained by summing $\rho_{\alpha n}(\zeta)$ over all Landau levels.

Spectral tailing into neighboring levels introduces additional contributions to ODT as was discussed in the Introduction. The first term of (8) [$\propto\rho_{vn}(\zeta)\rho_{cn}(\omega-\zeta)$] re-

sults from a direct $n \rightarrow n$ coupling of the electronic system with the photon field as is indicated by solid downward arrows with wiggly curves in Figs. 3(a) and 3(b) for $0 \rightarrow 0$ and $1 \rightarrow 1$ coupling, respectively. In these DT the majority of the photons emitted have energy close to $\epsilon_{cn} + \epsilon_{vn} + \epsilon_{\text{gap}}$. These DT correspond to the solid arrows directed downward in Fig. 1. The spectral-density function ρ_{c0} (ρ_{v1}) in Fig. 3(a) [Fig. 3(b)] has a secondary peak ($\propto \xi^2$) at the level $n_c = 1$ ($n_v = 0$), allowing photons (dashed lines directed downward in Fig. 3) to be emitted at the energy $\varepsilon_{c1} + \varepsilon_{v0} + \varepsilon_{\text{gap}}$. This process corresponds to the $1 \rightarrow 0$ transition. Although these processes originate from a direct $n \rightarrow n$ coupling with the photon field, they will be defined as ODT since they emit ODT photons. A similar inter-Landau-level scattering effect was noted to induce subharmonics of cyclotron resonance earlier.[7] The ODT process in Fig. 3(c) corresponds to that in Fig. 2 and to the second term in the square brackets of (8). In this process, primary spectral densities (ρ_{c1} and ρ_{v0}) at the levels $n_c = 1$ and $n_v = 0$ are utilized unlike in Figs. 3(a) and 3(b) but the admixing impurity matrix elements (see Fig. 2) are of the order of ξ^2.

IV. NUMERICAL EVALUATION

In this section we evaluate luminescence and excitation line shapes using the results in (1) and (6) for a symmetric $In_{0.2}Ga_{0.8}As/GaAs$ quantum well with 80 Å well width, 50-Å undoped GaAs spacer layers, 80-Å ionized doping layers, and $N = 8 \times 10^{11}$ cm^{-2}. This carrier density yields the Fermi energy of 27.4 meV for $m_c^*/m_0 = 0.07$ (in units of free-electron mass). At $B = 11$ T, level $n = 1$ in the conduction band is half filled. Cyclotron energies are given by 18.26 and 9.13 meV for electrons and holes with $m_v^*/m_0 = 0.14$[2]. Small mass differences between the quantum well and the barriers are ignored. The perpendicular masses (in the growth direction) equal 0.07 and 0.35 for electrons and holes, respectively. The confinement wave functions are given by symmetric variational wave functions with a cosine function in the well and evanescent expotentials in the barriers and with the coefficients chosen to minimize the energy. Hartree and local exchange-correlation potentials are used.[1] Band offsets for conduction and valence bands are given by 160 and 67 meV, respectively.[1] The damping constants are obtaining through $(\Gamma_{nm}^{\alpha})^2 = 4\langle n | U^{\alpha\alpha} | m \rangle$. The right-hand side of this equation contains the damping constants through the density of states in the polarizability Π_q [cf. (3c)] of the dielectric screening constant ε_q. Therefore the damping constants are calculated self-consistently through iteration to an arbitrary accuracy. Alloy scattering is estimated to contribute less than 1-meV widths to the Landau levels and is ignored.

A total of the four lowest Landau levels are considered for the basis set for calculating the luminescence line shape. Using the three lowest levels as a basis set gives the same result, indicating a rapid convergence of the result. For the excitation line shape, the lowest seven Landau levels are used as a basis set. Using the five lowest levels as a basis set yields the same result, again indicating a rapid convergence of the result. The line shapes calculated from (1) and (6) for luminescence and excitation are shown in Figs. 5 and 6, respectively.

For the luminescence spectra in Fig. 5, the $1 \rightarrow 0$ transition, prominent at 4 K, diminishes at 76 K where the new $1 \rightarrow 1$ transition shows a large intensity at the expense of the $0 \rightarrow 0$ intensity. The relative peak height of the $1 \rightarrow 1$ transition to that of the $0 \rightarrow 0$ transition at 76 K is determined by the Boltzmann distribution. On the other hand, the peak intensity of the $1 \rightarrow 0$ transition at 4 K is determined mainly by the matrix elements of the impurity potentials between the Landau-level states $n = 0$ and $n = 1$ and impurity-induced Landau-level spectral-density tailing. It should be mentioned here that the result at 76 K is calculated by using the zero-temperature screening formula in (3a) which underestimates the Coulomb interaction and the level widths somewhat at this high temperature.

For the excitation spectra in Fig. 6, the solid curve indicates the total ladder contribution. The satellite lines due to ODT appear below the $1 \rightarrow 1$ threshold as well as between the DT lines. DT and ODT are illustrated in Fig. 1 by solid and dashed arrows, respectively. The energy separation between the electron Landau levels is about twice that of the hole levels because $m_v^* \approx 2m_c^*$. The $1 \rightarrow 1$ peak is smaller than the $2 \rightarrow 2$ peak because the $n = 1$ electron level is half filled. It is clear from Fig. 1 that the excitation resonance peaks are approximately equally spaced in energy as shown in Fig. 6. These behaviors are consistent with the discussions presented in the Introduction. The relative strengths of ODT luminescence and excitation peaks are expected to increase with respect to those of DT for decreasing fields.

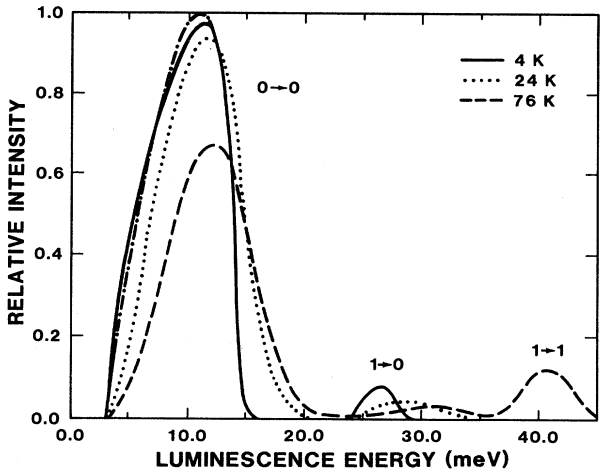

FIG. 5. Luminescence line shapes calculated from (1) and (6) at three different temperatures. The Fermi level is at the electron level $n = 1$, which is half filled. The parameters used are given in the text. The numbers connected by an arrow denote the initial conduction- and valence-band Landau levels responsible for the transition (see Fig. 1). The one-rung approximation shows a small deviation only for $0 \rightarrow 0$ peak at 4 K as shown by a dash-dotted curve.

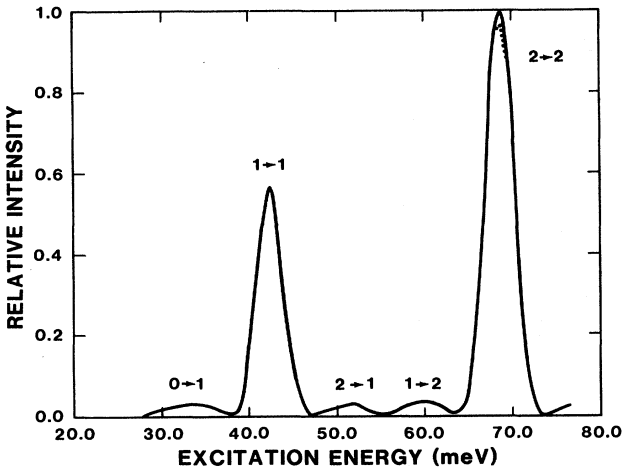

FIG. 6. Excitation line shape calculated from (1) and (6) at 4 K for the parameters given in the text. The Fermi level is at the electron level $n=1$, which is half filled. The numbers connected by an arrow denote the initial valence- and conduction-band Landau levels responsible for the transition (see Fig. 1). The $1\rightarrow 1$ transition is the usual threshold. The one-rung approximation shows a small deviation only for $2\rightarrow 2$ peak as shown by a dotted curve.

Measurement of the excitation line shapes in strong fields is in progress.[8]

We have also evaluated the line shapes using the one-rung result in (8). The line shapes show no significant differences from the ladder results except for small deviations for the $0\rightarrow 0$ 4 K luminescence peak (dash-dotted curve) in Fig. 5 and $2\rightarrow 2$ excitation peak (dotted curve) in Fig. 6.

V. CONCLUSIONS

A theory of luminescence and excitation line-shape function was developed in a strong magnetic field. The effect of carrier-impurity interactions on luminescence and excitation line shapes was examined by summing the ladder diagrams exactly. The broadening and tailing of the Landau-level spectral density (essential for evaluating the spectroscopy line shape) was investigated by employing a self-consistent Born approximation which includes inter-Landau-level impurity scattering. The accuracy of the one-rung approximation was assessed and found to be fairly high, when the Fermi energy is much larger than the Landau-level widths. This is not surprising in view of the fact that a ladder approximation is important in dc transport problems where each successive rung introduces overlapping resonances of a pair of Green's functions.[9] In the present problem, however, each rung introduces mainly virtual admixing of Landau-level states (responsible for ODT) as discussed in the Introduction. We found that carrier-impurity scattering not only broadens the line but yields breaking of the usual $n\rightarrow n$ selection rule, inducing ODT. As a result, the luminescence line shape crosses over from $n\rightarrow 0$ ($n=0,1,\cdot$) transitions at low temperatures to $n\rightarrow n$ transitions at high temperatures as observed recently.[2] For excitation spectra, carrier-impurity interactions induce new satellite lines corresponding to ODT below the threshold as well as between the main lines.

Another possible mechanism which can contribute to ODT lines are Auger-type processes[10] where a carrier is scattered off other carriers through Coulomb interactions. Since such processes are inelastic, ODT luminescence lines are expected to be seen below the main $0\rightarrow 0$ line as well as above it in contrast to the elastic scattering case shown in Fig. 5. These processes have been ruled out in Ref. 2 on the basis of data.

ACKNOWLEDGMENTS

The author thanks Dr. E. D. Jones for a critical reading of the manuscript and for valuable discussions on the subject. He thanks Dr. G. E. W. Bauer for calling his attention to Ref. 3. He is grateful to Dr. D. E. Amos for very helpful discussions on numerical analysis. This work was supported by the U.S. Department of Energy under Contract No. DE-AC04-76DP00789.

APPENDIX

In this Appendix we derive the self-energy part in Eq. (9) and the spectral density in the high-field limit where the Landau levels are well separated. The self-energy part is given in the self-consistent Born approximation by

$$S_{\alpha n}(z)=\tfrac{1}{4}\sum_m \frac{(\Gamma^{\alpha}_{nm})^2}{z-\epsilon_{\alpha m}-S_{\alpha m}(z)} \ . \tag{A1}$$

The symbols used in (A1) are defined in the text. The diagonal contribution ($m=n$) arises from intra-Landau-level impurity scattering and the off-diagonal contribution ($m\neq n$) from inter-Landau-level scattering. Denoting the self-energy part as $S^0_{\alpha n}(z)$ when the energy z lies inside the (broadened) Landau level n, we find

$$S^0_{\alpha n}(z)=\frac{1}{4}\frac{(\Gamma^{\alpha}_{nn})^2}{z-\epsilon_{\alpha n}-S^0_{\alpha n}(z)}+\delta_{\alpha n}(z) \ , \tag{A2}$$

where $\delta_{\alpha n}$ is defined in (9d). At this stage the self-energy part is dropped from the denominator of $\delta_{\alpha n}$ in the right-hand side of (9d), being much smaller than the cyclotron energy. Solving (A2) for $S^0_{\alpha n}$, we find for ζ inside the nth level (i.e., $A_{\alpha n}\geq 0$)

$$S^0_{\alpha n}(\zeta-i0)=\tfrac{1}{2}(\zeta-\epsilon_{\alpha n}+\delta_{\alpha n}+i\sqrt{A_{\alpha n}}) \ , \tag{A3}$$

where $A_{\alpha n}$ is defined in (9c).

When the energy z lies inside another Landau level $m\neq n$ (i.e., $A_{\alpha m}\geq 0$), (A1) is rewritten as

$$S_{\alpha n}(z)=\frac{1}{4}\frac{(\Gamma^{\alpha}_{nn})^2}{z-\epsilon_{\alpha n}-S_{\alpha n}(z)}+\Delta_{nm}(z) \ , \tag{A4}$$

where

$$\Delta_{nm}(z)=\frac{1}{4}\frac{(\Gamma^{\alpha}_{nm})^2}{z-\epsilon_{\alpha m}-S^0_{\alpha m}(z)}+\tfrac{1}{4}{\sum_l}'' \frac{(\Gamma^{\alpha}_{nl})^2}{z-\epsilon_{\alpha l}} \ . \tag{A5}$$

Here the double prime in the second term indicates excluding $l=n,m$ from the summation. The second term is much smaller than the first term and is discarded. We then find from (A2), (A4), and (A5) for $A_{\alpha m} \geq 0$

$$S_{\alpha n}(z)=(\Gamma^{\alpha}_{nm}/\Gamma^{\alpha}_{mm})^2 S^0_{\alpha m}(z) , \tag{A6}$$

which, combined with (A3), yields (9a).

The total number of states inside a given (say, nth) Landau level is obtained by integrating the density of states in the entire region where $A_{\alpha n}(\zeta)\geq 0$. We find from (9) and (5)

$$\frac{1}{\pi}\sum_m \int \Theta(A_{\alpha n}(\zeta))I_{\alpha m}(\zeta)d\zeta=1 \tag{A7}$$

to the order $\xi^2_{\alpha n}$ ($\ll 1$) where

$$\xi^2_{\alpha n}=\tfrac{1}{4}\sum_m{}' \frac{(\Gamma^{\alpha}_{nm})^2}{(\epsilon_{\alpha n}-\epsilon_{\alpha m})^2} . \tag{A8}$$

Use is made of the relationship

$$(\Gamma^{\alpha}_{nn})^{-2}\int \Theta(A_{\alpha n})\sqrt{A_{\alpha n}}d\zeta=\frac{\pi}{2}(1+\xi^2_{\alpha n})^{-1} . \tag{A9}$$

The spectral density of any Landau level n satisfies the normalization condition:

$$\frac{1}{\pi}\int_{-\infty}^{\infty} I_{\alpha n}(\zeta)d\zeta=(1+\xi^2_{\alpha n})^{-1}+\xi^2_{\alpha n}\approx 1 . \tag{A10}$$

The first (second) term following the first equality represents the total integrated spectral density from inside (outside) the level n reduced (induced) by the inter-Landau-level scattering by the amount $\xi^2_{\alpha n}$. This special-density tailing effect is schematically illustrated in Fig. 3.

[1]S. K. Lyo and E. D. Jones, Phys. Rev. B **38**, 4113 (1988).
[2]S. K. Lyo, E. D. Jones, and J. F. Klem, Phys. Rev. Lett. **61**, 2265 (1988).
[3]G. E. W. Bauer and T. Ando, J. Phys. C **19**, 1553 (1986).
[4]H. Scher and T. Holstein, Phys. Rev. **148**, 598 (1966).
[5]Y. Murayama and T. Ando, Phys. Rev. B **35**, 2252 (1987).
[6]For small q, this quantity becomes linear in q and its coefficient is small when the electron and hole have similar distributions.
[7]T. Ando, J. Phys. Soc. Jpn. **39**, 989 (1975); T. Ando, A. B. Fowler, and F. Stern, Rev. Mod. Phys. **54**, 437 (1982).
[8]E. D. Jones (private communication).
[9]T. Holstein, Ann. Phys. (N.Y.) **29**, 410 (1964).
[10]A. E. Ruckenstein and S. Schmitt-Rink, Phys. Rev. B **35**, 7551 (1987).